RAD51 Haploinsufficiency Causes Congenital Mirror Movements in Humans

Christel Depienne,[1,2,3,4,5] Delphine Bouteiller,[1,2,4,5] Aurélie Méneret,[1,6] Ségolène Billot,[7] Sergiu Groppa,[8] Stephan Klebe,[1,2,3,4,8,9] Fanny Charbonnier-Beaupel,[1,2,4] Jean-Christophe Corvol,[1,2,4,9] Jean-Paul Saraiva,[10] Norbert Brueggemann,[11] Kailash Bhatia,[12] Massimo Cincotta,[13] Vanessa Brochard,[9] Constance Flamand-Roze,[14] Wassila Carpentier,[15] Sabine Meunier,[1] Yannick Marie,[1,4,5] Marion Gaussen,[1,2,4] Giovanni Stevanin,[1,2,3,4,16] Rosine Wehrle,[17,18] Marie Vidailhet,[1,2,4,6] Christine Klein,[11] Isabelle Dusart,[17,18] Alexis Brice,[1,2,3,4,21,*] and Emmanuel Roze[1,4,6,19,20,21]

Congenital mirror movements (CMM) are characterized by involuntary movements of one side of the body that mirror intentional movements on the opposite side. CMM reflect dysfunctions and structural abnormalities of the motor network and are mainly inherited in an autosomal-dominant fashion. Recently, heterozygous mutations in *DCC*, the gene encoding the receptor for netrin 1 and involved in the guidance of developing axons toward the midline, have been identified but CMM are genetically heterogeneous. By combining genome-wide linkage analysis and exome sequencing, we identified heterozygous mutations introducing premature termination codons in *RAD51* in two families with CMM. *RAD51* mRNA was significantly downregulated in individuals with CMM resulting from the degradation of the mutated mRNA by nonsense-mediated decay. RAD51 was specifically present in the developing mouse cortex and, more particularly, in a subpopulation of corticospinal axons at the pyramidal decussation. The identification of mutations in *RAD51*, known for its key role in the repair of DNA double-strand breaks through homologous recombination, in individuals with CMM reveals a totally unexpected role of *RAD51* in neurodevelopment. These findings open a new field of investigation for researchers attempting to unravel the molecular pathways underlying bimanual motor control in humans.

Mirror movements (MM) are involuntary movements of one side of the body that mirror intentional movements on the opposite side. Mild MM are physiological in young children and gradually disappear within the first decade of life probably because of the maturation of the motor network.[1] Congenital mirror movements (CMM [MIM 157600]) persisting after age 10 in subjects with no other clinical feature constitute a rare disorder that is mainly inherited in an autosomal-dominant fashion although sporadic cases also exist. MM predominate in the upper limbs, with muscles controlling the fingers and hands being constantly involved, and their intensity increases with the complexity of the voluntary movement. MM impair the ability to perform tasks requiring skilled bimanual coordination and are associated with pain in the upper limbs during sustained manual activities. In this setting, MM reflect multiple dysfunctions and structural abnormalities of the motor network, including altered decussation of the corticospinal tracts.[2]

Recently, heterozygous mutations in *DCC* (deleted in colorectal carcinoma [MIM 120470]), the gene encoding the receptor for netrin 1 (*NTN1* [MIM 601614]), have been identified in families with autosomal-dominant CMM.[3,4] Impairment of DCC/netrin 1 signaling, which promotes attraction and guidance of developing axons toward the midline, results in alterations of axonal fiber crossing and abnormal ipsilateral connections.[3,4] MM are genetically heterogeneous, however; no *DCC* mutations have been identified in several familial and sporadic cases.[4,5]

We have previously ruled out *DCC* mutations in a French family (Family A) with autosomal-dominant MM.[4] Written informed consent was obtained from all patients before blood sampling. The study received approval from ethical standards committee on human experimentation (INSERM, CHU Pitié-Salpêtrière). Genome-wide linkage analysis with SNP microarrays followed by genotyping with 92 microsatellite markers on uninformative or positive regions in this family identified a single linked region with a maximal multipoint LOD score value (+2.4) in chromosome region 15q14-q21.2 (Figure 1A). A common haplotype, delimited by markers D15S102 and D15S982

[1]INSERM, U975 - CRICM, Hôpital Pitié-Salpêtrière, 75013 Paris, France; [2]CNRS 7225 - CRICM, Hôpital Pitié-Salpêtrière, 75013 Paris, France; [3]AP-HP, Hôpital Pitié-Salpêtrière, Département de Génétique et de Cytogénétique, Centre de Génétique Moléculaire et Chromosomique, 75013 Paris, France; [4]Université Pierre et Marie Curie-Paris-6, UMR_S 975, 75013 Paris, France; [5]ICM, PFGS Platform, Hôpital Pitié-Salpêtrière, 75013 Paris, France; [6]AP-HP, Hôpital Pitié-Salpêtrière, Département de Neurologie, 75013 Paris, France; [7]AP-HP, Hôpital Avicenne, Service de Neurologie, 93000 Bobigny, France; [8]Department of Neurology, University Hospital Schleswig-Holstein, Campus Kiel, 24105 Kiel, Germany; [9]INSERM, AP-HP, Centre d'Investigation Clinique 9503, 75013 Paris, France; [10]Integragen SA, 91000 Evry, France; [11]Section of Clinical and Molecular Neurogenetics, Department of Neurology, University of Luebeck, 23538 Luebeck, Germany; [12]Sobell Department of Motor Neuroscience and Movement Disorders, Institute of Neurology, UCL, London, WC1N 3BG, UK; [13]Unità Operativa di Neurologia, Azienda Sanitaria di Firenze, Ospedale San Giovanni di Dio, 50124 Firenze, Italy; [14]AP-HP, Hôpital de Bicêtre, Service de Neurologie, 94275 Paris, France; [15]P3S Platform, Hôpital Pitié-Salpêtrière, 75013 Paris, France; [16]Ecole Pratique des Hautes Etudes, 75007 Paris, France; [17]CNRS, UMR 7102, 75005 Paris, France; [18]UPMC Univ Paris 06, UMR 7102, 75005 Paris, France; [19]INSERM, UMRS 952, 75013 Paris, France; [20]CNRS, UMR 7224, 75005 Paris, France
[21]These authors contributed equally to this work
*Correspondence: alexis.brice@upmc.fr
DOI 10.1016/j.ajhg.2011.12.002.

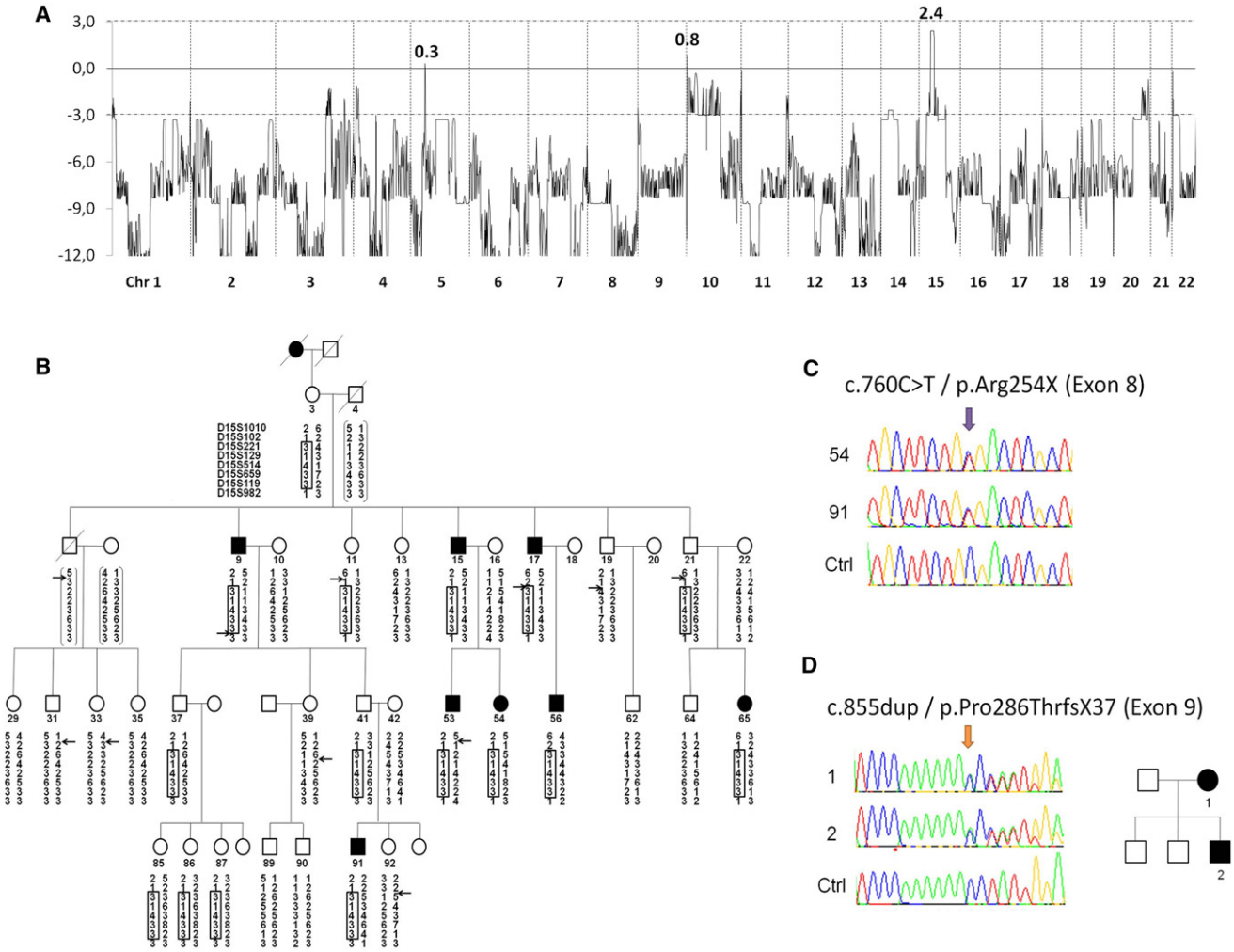

Figure 1. Identification of *RAD51* Mutations in Two Independent Families

(A) LOD score plot for genome-wide linkage analysis in Family A, revealing a single locus with a maximal multipoint LOD score value on chromosome arm 15q (Z = +2.4). Twenty-six family members (7 symptomatic individuals, 3 obligate carriers, 12 at-risk asymptomatic relatives, and 4 spouses) were genotyped by linkage-24 microarrays (Illumina). Multipoint LOD scores were calculated with Merlin 1.0 (affected-only analysis, autosomal-dominant trait, disease allele frequency of 0.00001, penetrance of 80%, null phenocopy rate). All regions with LOD scores >−2 other than that on chromosome 15 were further analyzed with microsatellite markers and excluded on the basis of the absence of a common haplotype in all affected family members.

(B) Refinement of the chromosome 15 interval with eight microsatellite markers (D15S1010, D15S102, D15S221, D15S129, D15S514, D15S659, D15S119, D15S982) showing a common haplotype segregating in all affected family members. Multipoint LOD scores were recalculated from the microsatellite markers in the chromosome 15 interval via Allegro 1.0 with the same parameters as those previously used (Zmax = +2.7).

(C) Confirmation of the c.760C>T (p.Arg254*) mutation in *RAD51* by Sanger sequencing in Family A.

(D) The coding region of *RAD51* was amplified with 11 primer pairs (sequences available on request) in the index cases of Families B (from Germany) and C (from UK). The c.855dupA (p.Pro286Thrfs*37) mutation in *RAD51* was identified in Family B (pedigree).

and encompassing a 14.4 Mb region, segregated in all eight affected family members and in eight asymptomatic relatives, including three obligate carriers. The multipoint LOD score, recalculated from microsatellite marker genotypes and including all eight affected members, reached +2.7, its maximal expected value in view of the pedigree structure (Figure 1B). The region contained 223 known genes, but only one, *SEMA6D* (MIM 609295), was potentially involved in neuronal migration. Direct sequencing of its coding sequence detected no mutations in Family A or in a second family (from Germany) with two affected members (Family B). In addition, analysis of the Family A proband by high-resolution CGH array (Nimblegen HD-2 microarrays, Roche) revealed no microdeletion or duplication within the candidate interval.

We then sequenced the entire exome in two affected members of Family A (individuals 54 and 91). A total of 32,390 and 33,648 variants were identified in each subject (Table S2 available online). Further analysis focused on the eight variants (five SNPs and three indels) that were (1) heterozygous in the two affected subjects, (2) absent from the dbSNP database (version 132), and (3) contained in the linked interval (Table 1). Seven variants were confirmed by Sanger sequencing, four of which were also

Table 1. List of the Variants Detected by Whole-Exome Analysis that Are Present in Patients 54 and 91 from Family A, Located in the Chromosome 15 Interval, and Absent from the dbSNP Database

Position on chr15 (in bp)	Gene	RefSeq Accession Number/MIM Number	Exon/ Intron	Nucleotide Change	Protein Change	Type	Status in 54	Status in 91	Confirmation by Sanger[a]	In Silico Prediction[b]	Presence in Controls[c]	Expression in Brain
38543560	*BAHD1*	NM_014952/613880	intron 4	c.1975+49A>C	-	intronic	htz	htz	yes	NE	0/321	yes
38809110	*RAD51*	NM_002875/179617	exon 8	c.760C>T	p.Arg254*	nonsense	htz	htz	yes	-	0/644	yes
38817215	*FAM82A2*	NM_018145/611873	exon 10	c.1127T>G	p.Val376Gly	missense	htz	htz	no	-	-	-
40164933	*PLA2G4D*	NM_178034/612864	intron 5	c.428+45_ 428+48dup	-	intronic	htz	htz	yes	NE	21/92	yes
40167192	*PLA2G4D*	NM_178034/612864	intron 1	c.46-2del	-	intronic	htz	htz	yes	Decreases the score of the acceptor splice site	4/356	yes
40221690	*PLA2G4F*	NM_213600/-	exon	c.2334G>C	p.Val778Val	synonymous	htz	htz	yes	NE	2/93	yes
40241144	*VPS39*	NM_015289/612188	intron 24	c.2552+28del	-	intronic	htz	htz	yes	NE	21/91	yes
40481666	*CAPN3*	NM_000070/114240	intron 12	c.1536+41C>T	-	intronic	htz	htz	yes	NE	0/334	yes

Genomic positions were based on the the NCBI36/hg18 version of the Human genome. Abbreviations: htz, heterozygous; NE, no major effect on splicing.
[a] The eight variants were confirmed by Sanger sequencing: yes, the variant was present in both individuals; no, the c.1127T>G (p.V376G) variant was absent from both individuals.
[b] In silico predictions were assessed for intronic variants via Alamut 2.0 (Interactive Biosoftware, Rouen, France).
[c] Number of individuals with the variant/total number of controls tested.

found in control individuals. The three remaining variants included two intronic substitutions predicted to have no effect on splicing, and a nonsense mutation (c.760C>T [p.Arg254*], RefSeq accession number NM_002875) in exon 8 of *RAD51* (MIM 179617). This nonsense mutation cosegregated with MM in Family A (Figure 1C) and was absent from 644 healthy unrelated European individuals.

As an alternative method to identify the mutated gene in Family A, we searched for deregulated genes in lymphoblasts from affected subjects. Reverse-transcribed RNA from lymphoblasts of four affected subjects and three unaffected noncarrier relatives of Family A were hybridized on Illumina HumanHT-12 beadchips. Two independent statistical analyses restricted to genes contained in the chromosome 15 interval showed that *RAD51* mRNA was significantly downregulated in affected versus control individuals (fold difference = 0.7, $p = 0.009$; Table 2; Figures 2A–2C). By pretreating the lymphoblastic cells of affected members of Family A with emetin, we demonstrated that this downregulation corresponded to the degradation of the mutated mRNA by nonsense-mediated decay (Figure 2D). In addition, no truncated protein could be observed in western blot analysis in untreated lymphoblastic cells of three affected family members (not shown).

To confirm that mutations in *RAD51* can cause MM, we screened the *RAD51* coding sequence by Sanger sequencing in the index cases of Family B and of a third family from the UK in which point mutations in *DCC* had been ruled out (Family C). Duplication of an adenine (c.855dupA), introducing a premature termination codon (p.Pro286Thrfs*37), was identified in exon 9 of *RAD51* in Family B (Figure 1D) and was absent from the 644 control subjects. No mutation was identified in Family C. Altogether, these results show that heterozygous mutations introducing premature termination codons in *RAD51* cause congenital mirror movements in two unrelated families. Because *RAD51* mRNA was significantly downregulated in individuals with CMM of Family A resulting from the degradation of the mutated mRNA by nonsense-mediated decay, haploinsufficiency is the main consequence of the mutations and the disease probably occurs once the amount of functional RAD51 falls below a critical level.

RAD51 is essential for maintaining genomic integrity through its involvement in the repair of DNA double-strand breaks by homologous recombination (HR).[6–8] The RAD51 protein interacts with BRCA1 (*BRCA1* [MIM 113705]) and BRCA2 (*BRCA2* [MIM 600185])[9–11] and defective HR is predicted to contribute to genomic instability and tumor development. Therefore, mutations in *RAD51* have long been predicted to increase the risk of developing cancers[12] or to modulate the tumor response or resistance to chemotherapy.[13,14] However, a single constitutional missense variant was reported in two siblings with breast cancer, indicating that *RAD51* is not a major cancer predisposition gene.[15] Our findings are

Table 2. Classic Class Comparison Analysis of Transcriptomic Data between Affected Individuals and Controls

Unique Illumina ID	Gene (MIM Number)	Fold-Change Controls/Patients	Parametric p Value	Controls Gene Expression	Patients Gene Expression	Expression in Brain
ILMN_1794157	*CATSPER2P1* (-)	1.51	0.002	172.77	114.67	-
ILMN_1697629	*PLA2G4B* (606088)	1.52	0.005	541.34	356.32	-
ILMN_2363027	*RAD51* (179617)	1.42	0.009	200.72	141.79	+
ILMN_2372379	*MGA* (-)	1.24	0.009	78.27	63.15	+
ILMN_2401906	*CDAN1* (607465)	1.31	0.014	11358.92	8684.88	+
ILMN_1710329	*MYEF2* (-)	1.96	0.030	23.11	11.8	+

RNA extracted from lymphoblasts of four affected individuals and three spouses were hybridized on Illumina HumanHT12 beadchips. Expression profiles were extracted and normalized with Beadstudio software (Illumina). Normalized expression data were log2 transformed. The 131 genes expressed on bead chips from the 223 candidate genes on chromosome 15 were included for further analysis. Genes differently expressed between affected individuals and controls were selected for a fold difference of at least 1.2 between groups and a univariate p value of 0.05 with BRB array tools software. Six genes were significantly underexpressed in the affected individuals compared to the controls ($p < 0.05$, fold-change > 1.2), four of which were expressed in the brain (expression data provided by Genecards). No correction for multiple comparisons was used because the number of samples was too small and because this gene list would be intersected with the second approach (Figure 2A).

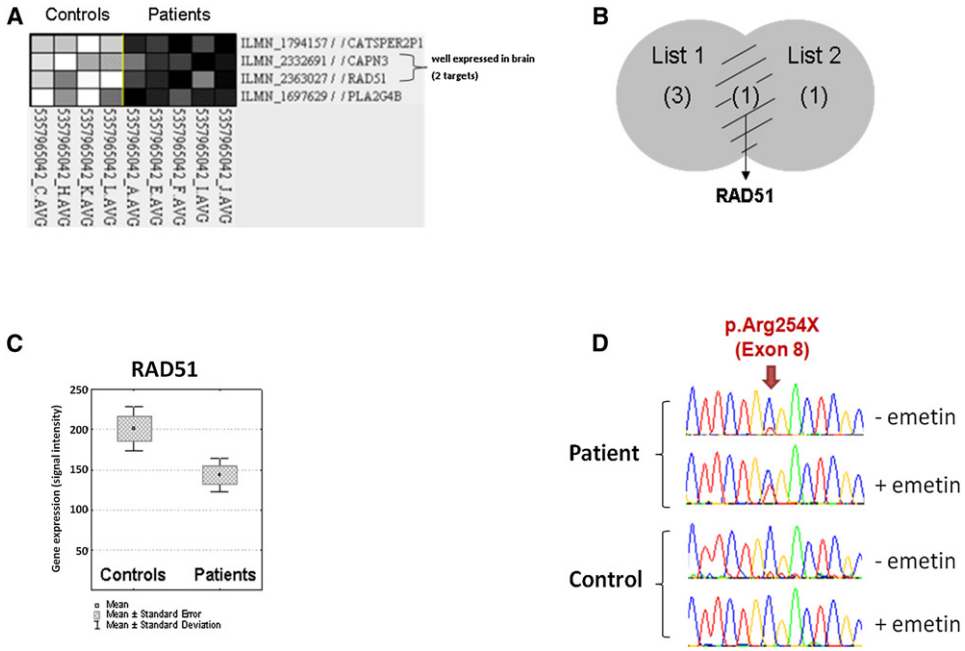

Figure 2. Downregulation of *RAD51* mRNA in Lymphoblasts from Affected Individuals and Degradation of the Mutated mRNA by Nonsense-Mediated Decay

In parallel with the whole-exome analysis, we used transcriptomic analysis to identify the gene responsible for MM in Family A, postulating that the mutation might decrease the mRNA expression in lymphoblasts from affected individuals compared to healthy spouses from the same family. Total RNA extracted from lymphoblasts of four affected individuals and three spouses were hybridized on lllumina HumanHT12 beadchips. Expression profiles were extracted and normalized with Bead studio software (Illumina). Normalized expression data were log2 transformed. The 131 genes expressed on bead chips from the 223 candidate genes on chromosome 15 were included for further analysis. Two complementary statistical analyses by two independent investigators were performed to identify genes differentially expressed between the groups. Results of classic class comparison analysis are presented in Table 2.

(A) Gene clustering approach with the pattern discovery tool of GeneATWork software (IBM Research). The filtering criteria for a gene's inclusion in a pattern are a maximum deviation of 0.05 and a p value of 0.001. The best patterns classifying the "phenotype" and "control" groups were retained. This approach distinguished the affected individuals from the controls on the basis of four genes underexpressed in the affected subjects. Among these four genes (*CATSPER2P1, CAPN3, RAD51*, and *PLA2G4B*), only two (*RAD51* and *CAPN3*) were expressed in the brain.

(B) *RAD51* was the only gene lying at the intersection of the gene lists obtained with the two statistical analyses.

(C) Expression data obtained for *RAD51* on HumanHT12 beadchips.

(D) Lymphoblastic cells from three affected individuals and three asymptomatic spouses from Family A were treated overnight with 10 μg/ml emetin to inhibit nonsense-mediated decay (NMD). Total RNA was extracted with the QIAGEN RNeasy Mini kit (Invitrogen) and reverse-transcribed with the SuperScript III First-Strand Kit (Invitrogen). *RAD51* cDNA was amplified and sequenced with specific primers located in exons 7 (Forward) and 10 (Reverse). Chromatograms for one affected individual and one spouse, showing lower levels of mutated mRNA compared to WT mRNA in untreated cells and a comparable expression levels of both mRNA in cells pretreated with emetin, are shown.

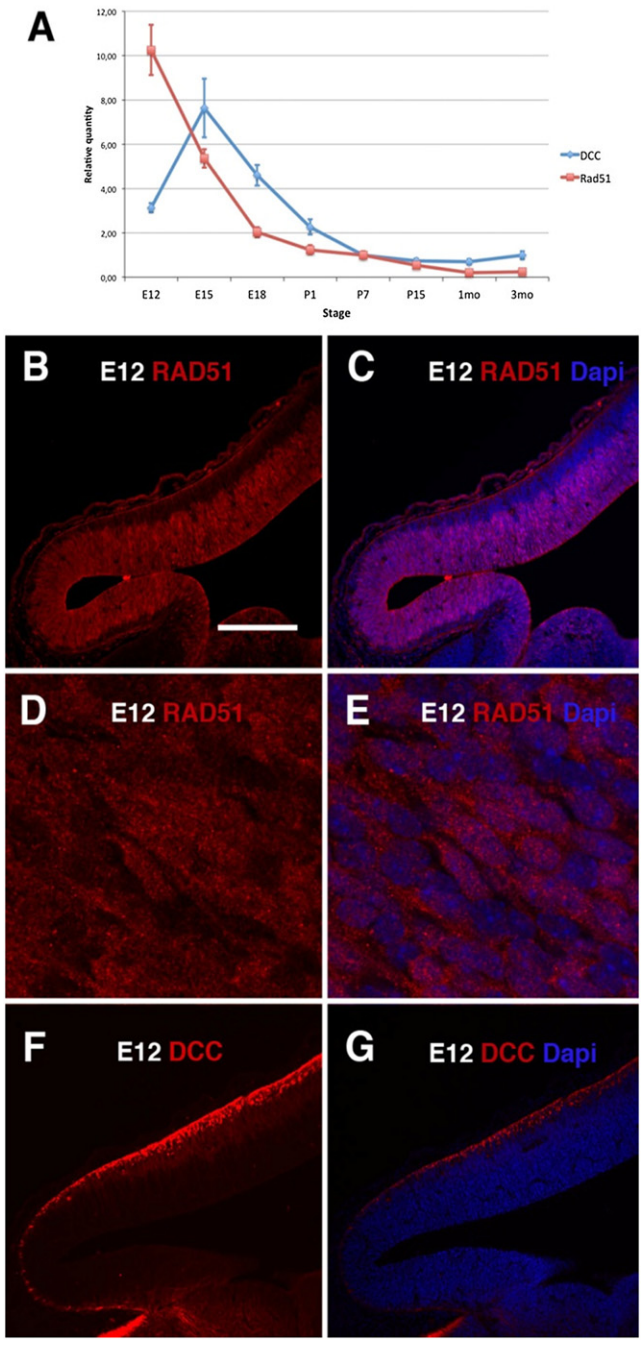

Figure 3. Comparative Expression and Localization of RAD51 and DCC in Developing Mouse Cortex

(A) Quantification of *RAD51* and *DCC* expression in mouse cerebral cortex sampled in quadruplicate at several stages of development (E12, E15, E18, P1, P7, P15, 1 month, and 3 months) by real-time PCR. Quantification of each sample was carried out with the QIAGEN QuantiTect primer assays for *DCC* and *RAD51*. *PPIA* and *PGK1* were used as control genes. Each sample was run in triplicate on a Lightcycler-1536 apparatus (Roche). Forty-five two-step cycles (15 s at 95°C and 30 s at 60°C) were performed. Analysis was performed with qbase Plus software (Biogazelle).

(B–G) Sagittal sections of the neocortex of E12 mouse embryos, fixed overnight in paraformaldehyde 4%, and immunolabeled with anti-RAD51 (1/50, sc-6862, Santa Cruz Biotechnology, Santa Cruz, CA) (B–E) or anti-DCC (1/100, sc-6535, Santa Cruz) (F and G) and counterstained with DAPI (C, E, G). Confocal plane (D, E). Scale bar represents 220 μm (B, C, F, G) or 15 μm (D, E).

consistent with this observation and reveal an unexpected role of this gene in mammalian neurodevelopment.

To gain further insight into this function and to identify a possible relationship between *RAD51* and *DCC*, we compared the expression of the two genes in the developing mouse cortex. *DCC* expression increased from embryonic day 12 (E12) to embryonic day 15 (E15), whereas *RAD51* expression was strongest at E12; expression of both genes declined thereafter (Figure 3A). The spatial distribution of RAD51 was different from that of DCC and evolved during brain development: at E12, RAD51 was mostly detected in the cortical ventricular zone (proliferative zone; Figures 3B and 3C), whereas DCC was present in the preplate (postmitotic zone; Figures 3F and 3G), confirming previous observations.[16,17] In the cortex of newborn mice (P0), RAD51 was mainly present in the subplate (SP) and, in lesser amounts, in layer V (Figures 4A and 4B), whereas DCC was selectively located in axons innervating the cortex (Figures 4C, 4D, 4G, and 4H). Strikingly, RAD51 was detected in a subpopulation of corticospinal axons at the pyramidal decussation in 2-day-old (P2) mice (Figures 4I and 4J), suggesting that *RAD51* deficiency could specifically alter the decussation process. *RAD51* is therefore specifically present in the developing mouse cortex, in brain tissues and at stages that are critical for the establishment of the corticospinal tract.

Interestingly, the subcellular location of RAD51 also changed with the stage of development: RAD51 was mostly detected in the nucleus of progenitor cells at E12 (Figures 3D and 3E) whereas it was mainly localized in the cell soma in the subplate at P0 (Figures 4E and 4F) and had a punctiform distribution at the pyramidal decussation in P2 mice (Figures 4I′ and 4J′). These results suggest that RAD51 could have several functions related to different cellular localizations.

The precise mechanisms linking *RAD51* deficiency to MM are unclear, and the possible involvement of the DNA repair function in MM pathogenesis remains to be demonstrated. Insufficient *RAD51*-related DNA repair during early corticogenesis might lead to excessive apoptosis and altered central nervous system development, as observed in mice lacking *XRCC2*, another gene of the *RAD51* family also involved in HR-mediated DNA repair.[18,19] The location of RAD51 in the cytoplasm of cortical cells during mouse brain development, as previously described in other cell types, suggests, however, a role of RAD51 different from its function in HR occurring within the nucleus.[20] It might have a direct or indirect role in axonal guidance, as shown for *DCC*. In keeping with this hypothesis, high *RAD51* levels are associated with increased expression of genes involved in actin remodeling in nonneuronal cells.[21] Nevertheless, the different cellular locations of DCC and RAD51 during cortical development suggest that these proteins do not interact directly.

Interestingly, homozygous *Rad51*$^{-/-}$ rodent zygotes show altered cell proliferation and abnormal cell morphology and are unable to undergo embryonic

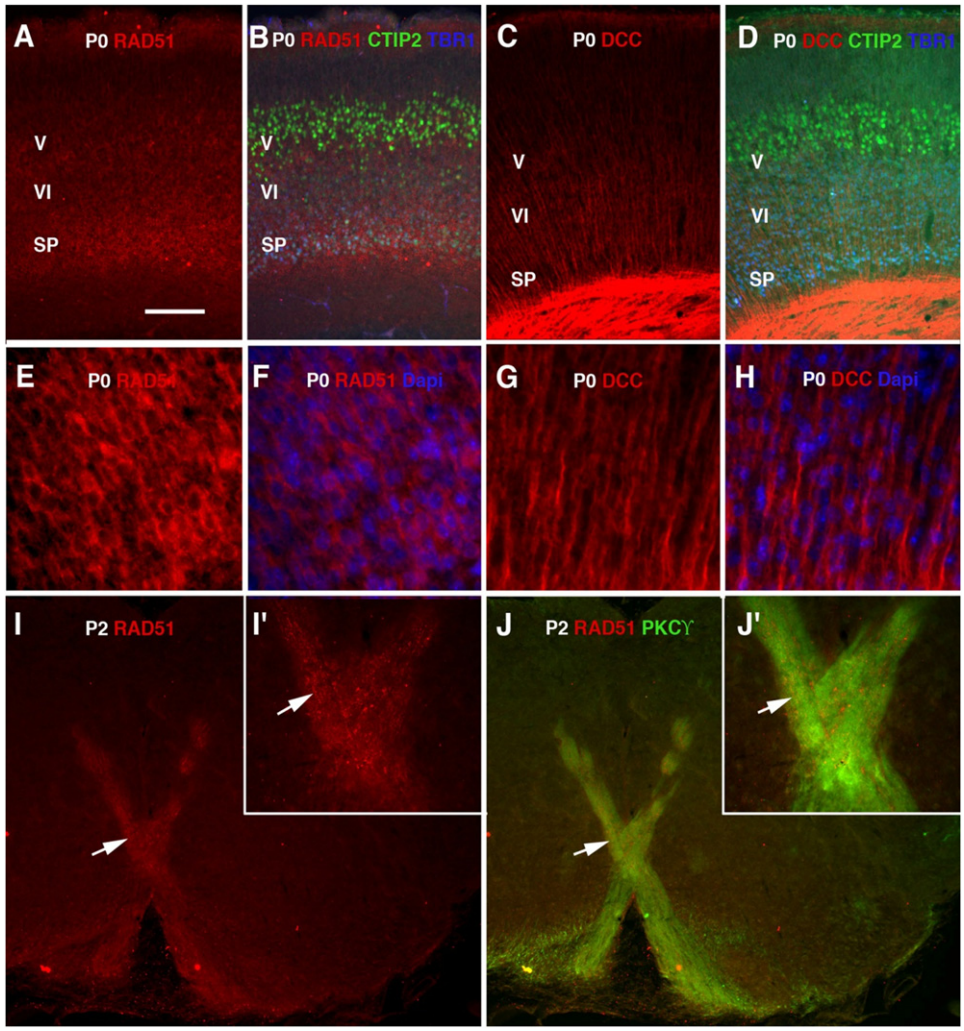

Figure 4. Comparative Localization of RAD51 and DCC in Mouse Brain at Postnatal Stages
(A–H) Cortical coronal section of a newborn (P0) mouse triple immunostained with anti-TBR1 (1/500, Millipore, Molsheim, France) to label the subplate and layer VI, anti-CTIP2 (1/500, Abcam, Cambridge, UK) to label layer V, and either anti-RAD51 (1/50, sc-6862, Santa Cruz) (A, B) or anti-DCC (1/100, sc-6535, Santa Cruz) (C, D), or immunolabeled only with anti-RAD51 (E, F) or anti-DCC (G, H) and counterstained with DAPI (F, H).
(I and J) Coronal section of a P2 mouse at the pyramidal decussation, immunostained with anti-RAD51 (I, J) and anti-PKCγ (1/100, sc211, Santa-Cruz) to label the corticospinal tract (J).
(I′ and J′) Enlargements of (I) and (J); arrows point to the same area.
Scale bar represents 120 μm (A–D), 30 μm (E–H), 250 μm (I, J), or 100 μm (I′, J′).

development after embryonic day 6.[22,23] Heterozygous *Rad51*$^{+/-}$ mice are viable, fertile, and appear normal in outer appearance, but neither the morphological organization of their central nervous system nor their motor phenotype has yet been investigated.[22,23] Therefore, it is currently unclear whether the *Rad51*$^{+/-}$ mice reproduce, at least in part, the human phenotype. Further characterization of mouse models is necessary to address this issue and to unravel the mechanisms by which *RAD51* mutation leads to mirror movements in humans.

A striking feature is the reduced penetrance associated with *RAD51* mutations: in Family A, 8 out of the 16 individuals with the p.Arg254* mutation were asymptomatic at examination, for a penetrance of 50%. The absence of mirror movements in these individuals could be, for example, due to a higher expression of *RAD51* from the remaining normal allele or to other genetic or epigenetic modifiers. Interestingly, embryonic development of *Rad51*$^{-/-}$ mice progressed further in a p53-null background, supporting the hypothesis that the genetic background modulates the phenotype induced by the *RAD51* mutation.[23] So far, *DCC* and *RAD51* seem to account for most MM families: over the four families studied in our laboratory, mutations in *DCC* were identified in one family[4] and mutations in *RAD51* were identified in two other families. One family (Family C) was negative for both genes but the existence of intragenic microrearrangements missed by sequencing was not tested and therefore it is uncertain whether a third gene responsible for MM exists.

Study of MM subjects or models provide a unique opportunity to investigate the network and mechanisms underlying the bimanual motor control, which are, so far largely unknown.[2] Our findings therefore open a field of investigation for researchers attempting to unravel the molecular pathways underlying bimanual motor control in humans.

Supplemental Data

Supplemental Data include two tables and can be found with this article online at http://www.cell.com/AJHG/.

Acknowledgments

We thank the families for their participation, the DNA and cell bank for DNA extraction and cell culture, Khadija Tahiri for RNA preparation, and Agnès Rastetter for technical support in western blot analysis. This work was supported by INSERM, by Djilalli Mehri, and by an unrestricted research grant from IPSEN. C.K. was supported by the Hermann and Lilly Schilling Foundation. M.C.'s unit was supported by Ente Cassa di Risparmio di Firenze.

Received: October 6, 2011
Revised: October 13, 2011
Accepted: December 7, 2011
Published online: February 2, 2012

Web Resources

The URLs for data presented herein are as follows:

BRB array tools software, http://linus.nci.nih.gov/BRB-ArrayTools.html
dbSNP database, http://www.ncbi.nlm.nih.gov/projects/SNP/
Genecards, http://www.genecards.org/
Online Mendelian Inheritance in Man (OMIM), http://www.omim.org

References

1. Bonnet, C., Roubertie, A., Doummar, D., Bahi-Buisson, N., Cochen de Cock, V., and Roze, E. (2010). Developmental and benign movement disorders in childhood. Mov. Disord. *25*, 1317–1334.
2. Galléa, C., Popa, T., Billot, S., Méneret, A., Depienne, C., and Roze, E. (2011). Congenital mirror movements: a clue to understanding bimanual motor control. J. Neurol. *258*, 1911–1919.
3. Srour, M., Rivière, J.B., Pham, J.M., Dubé, M.P., Girard, S., Morin, S., Dion, P.A., Asselin, G., Rochefort, D., Hince, P., et al. (2010). Mutations in DCC cause congenital mirror movements. Science *328*, 592.
4. Depienne, C., Cincotta, M., Billot, S., Bouteiller, D., Groppa, S., Brochard, V., Flamand, C., Hubsch, C., Meunier, S., Giovannelli, F., et al. (2011). A novel DCC mutation and genetic heterogeneity in congenital mirror movements. Neurology *76*, 260–264.
5. Djarmati-Westenberger, A., Brüggemann, N., Espay, A.J., Bhatia, K.P., and Klein, C. (2011). A novel DCC mutation and genetic heterogeneity in congenital mirror movements. Neurology *77*, 1580.
6. Park, J.Y., Yoo, H.W., Kim, B.R., Park, R., Choi, S.Y., and Kim, Y. (2008). Identification of a novel human Rad51 variant that promotes DNA strand exchange. Nucleic Acids Res. *36*, 3226–3234.
7. Li, X., and Heyer, W.D. (2008). Homologous recombination in DNA repair and DNA damage tolerance. Cell Res. *18*, 99–113.
8. West, S.C. (2003). Molecular views of recombination proteins and their control. Nat. Rev. Mol. Cell Biol. *4*, 435–445.
9. Jensen, R.B., Carreira, A., and Kowalczykowski, S.C. (2010). Purified human BRCA2 stimulates RAD51-mediated recombination. Nature *467*, 678–683.
10. Carreira, A., Hilario, J., Amitani, I., Baskin, R.J., Shivji, M.K., Venkitaraman, A.R., and Kowalczykowski, S.C. (2009). The BRC repeats of BRCA2 modulate the DNA-binding selectivity of RAD51. Cell *136*, 1032–1043.
11. Pellegrini, L., Yu, D.S., Lo, T., Anand, S., Lee, M., Blundell, T.L., and Venkitaraman, A.R. (2002). Insights into DNA recombination from the structure of a RAD51-BRCA2 complex. Nature *420*, 287–293.
12. Thacker, J. (2005). The RAD51 gene family, genetic instability and cancer. Cancer Lett. *219*, 125–135.
13. Klein, H.L. (2008). The consequences of Rad51 overexpression for normal and tumor cells. DNA Repair (Amst.) *7*, 686–693.
14. Slupianek, A., Schmutte, C., Tombline, G., Nieborowska-Skorska, M., Hoser, G., Nowicki, M.O., Pierce, A.J., Fishel, R., and Skorski, T. (2001). BCR/ABL regulates mammalian RecA homologs, resulting in drug resistance. Mol. Cell *8*, 795–806.
15. Kato, M., Yano, K., Matsuo, F., Saito, H., Katagiri, T., Kurumizaka, H., Yoshimoto, M., Kasumi, F., Akiyama, F., Sakamoto, G., et al. (2000). Identification of Rad51 alteration in patients with bilateral breast cancer. J. Hum. Genet. *45*, 133–137.
16. Ajioka, I., Maeda, T., and Nakajima, K. (2006). Identification of ventricular-side-enriched molecules regulated in a stage-dependent manner during cerebral cortical development. Eur. J. Neurosci. *23*, 296–308.
17. Shu, T., Valentino, K.M., Seaman, C., Cooper, H.M., and Richards, L.J. (2000). Expression of the netrin-1 receptor, deleted in colorectal cancer (DCC), is largely confined to projecting neurons in the developing forebrain. J. Comp. Neurol. *416*, 201–212.
18. Deans, B., Griffin, C.S., Maconochie, M., and Thacker, J. (2000). Xrcc2 is required for genetic stability, embryonic neurogenesis and viability in mice. EMBO J. *19*, 6675–6685.
19. Francis, F., Meyer, G., Fallet-Bianco, C., Moreno, S., Kappeler, C., Socorro, A.C., Tuy, F.P., Beldjord, C., and Chelly, J. (2006). Human disorders of cortical development: from past to present. Eur. J. Neurosci. *23*, 877–893.
20. Sage, J.M., Gildemeister, O.S., and Knight, K.L. (2010). Discovery of a novel function for human Rad51: maintenance of the mitochondrial genome. J. Biol. Chem. *285*, 18984–18990.
21. Orre, L.M., Fält, S., Szeles, A., Lewensohn, R., Wennborg, A., and Flygare, J. (2006). Rad51-related changes in global gene expression. Biochem. Biophys. Res. Commun. *341*, 334–342.
22. Tsuzuki, T., Fujii, Y., Sakumi, K., Tominaga, Y., Nakao, K., Sekiguchi, M., Matsushiro, A., Yoshimura, Y., and Morita, T. (1996). Targeted disruption of the Rad51 gene leads to lethality in embryonic mice. Proc. Natl. Acad. Sci. USA *93*, 6236–6240.
23. Lim, D.S., and Hasty, P. (1996). A mutation in mouse rad51 results in an early embryonic lethal that is suppressed by a mutation in p53. Mol. Cell. Biol. *16*, 7133–7143.